Direct Tests of Single-Parameter Aging. Supplementary Material.

Tina Hecksher, Niels Boye Olsen, Jeppe C. Dyre
DNRF Centre Glass and Time, IMFUFA, Department of Sciences, Roskilde University, Postbox 260, DK-4000 Roskilde, Denmark
(Dated: June 26, 2015)

I. LIQUIDS

Data for the following three liquids are used for the analysis in Figs. 1-4 of the paper: tetramethyl-tetrahpenyl-trisiloxane (DC704), 5-polyphenyl-4-ether (5PPE), tripropylene glycol (TPG). In this supplementary we also include data for triphenyl phosphite (TPP), dibutyl phthalate (DBP), diethyl phthalate (DEP), and 2,3-epoxy propyl-phenyl-ether (2,3-epoxy). A summary of relevant information about the liquids can be found in Table I.

All data can be found at the "Glass & Time" data repository

`http://glass.ruc.dk/data/`

II. METHODS

The setup, including a custombuilt cryostat, custombuilt voltage generator, commercial measuring electronics, and the prototype subcryostat (microregulator), is described in detail in Ref. 3 dealing with the cryostat and Ref. 4 dealing with the electronics.

The measurements of the dielectric constant used for monitoring the low-frequency dielectric loss, high-frequency dielectric constant (ϵ_∞), and the scans of the beta loss peak are fairly standard, except for an added Peltier element in direct contact with the measuring cell acting as a sub-cryostat [4]. This extra temperature control makes it possible both to make very fast temperature jumps and to keep the temperature stable within milliKelvin over weeks or as long as required.

Figure 1 below shows data examples of the measurement types used.

A. Mechanical resonance frequency

The mechanical resonance measurements use the Piezo-electric Shear Gauge (PSG) [5] in a one-disc version. This setup is in thermal contact with the microregulator for precise temperature control and the possibility of fast temperature changes. For these measurements there are two liquid layer (one on each side of the piezo-electric ceramic disc). The layers are approximately 0.5 mm thick. This makes the characteristic thermal equilibration time somewhat longer than the dielectric counterpart (around 10 s). This method was used already in Ref. 6.

The measured mechanical resonance frequency, f_{res}, of the piezo disc is related to the shear modulus, G_∞, of the liquid (assuming that there are no significant shear relaxations above ω_0) by

$$G_\infty = \rho d h \left(f_{res}^2 - F_{res}^2\right) / (2\pi)^2 \tag{1}$$

where ρ is the density of the piezoceramic, d is the thickness of the liquid layer, h is the thickness of the piezoceramic disc, and F_{res} is the resonance frequency of the empty axially clamped disc [6, 7].

In Fig. 1(a) the resonance frequency is the peak in the imaginary part of the measured capacitance. Below we demonstrate how this resonance frequency is determined in the aging measurements.

A series of isothermal scans during aging of the mechanical resonance of the piezo disc monitored via its electrical frequency-dependent capacitance are shown in Fig. 2(a) for four different temperatures close to and below the glass transition temperature ($T_g \approx 245$ K in this example, 5PPE). The resonance moves up in frequency over time as the sample equilibrates at the new (lower) temperature because the liquid shear modulus increases. In Fig. 2(b) the resonance frequency determined from the spectra is plotted as a function of time, showing clearly that with lower temperature, the equilibration takes longer and longer time.

A full frequency scan takes 13 minutes. For a sample that ages a data acquisition time as short as possible is preferred. The data presented in the paper are based on an algorithm for which it is only necessary to measure at two frequencies. This greatly reduces the scanning time and makes it possible to monitor even quite rapid changes. The method used for calculating the resonance frequency is based on the derivation given below, which makes use of the fact that the electrical impedance is zero at the resonance frequency. In the course of a measurement, the two frequencies monitored were adjusted to stay close to the resonance.

A simple resonance can be described by an LCR circuit, a series connection an inductor (L), a capacitor (C), and a resistor (R). The measured frequency-dependent (complex) capacitance J of this is given by

$$J = \frac{1}{\frac{1}{C} + i\omega R - \omega^2 L} \tag{2}$$

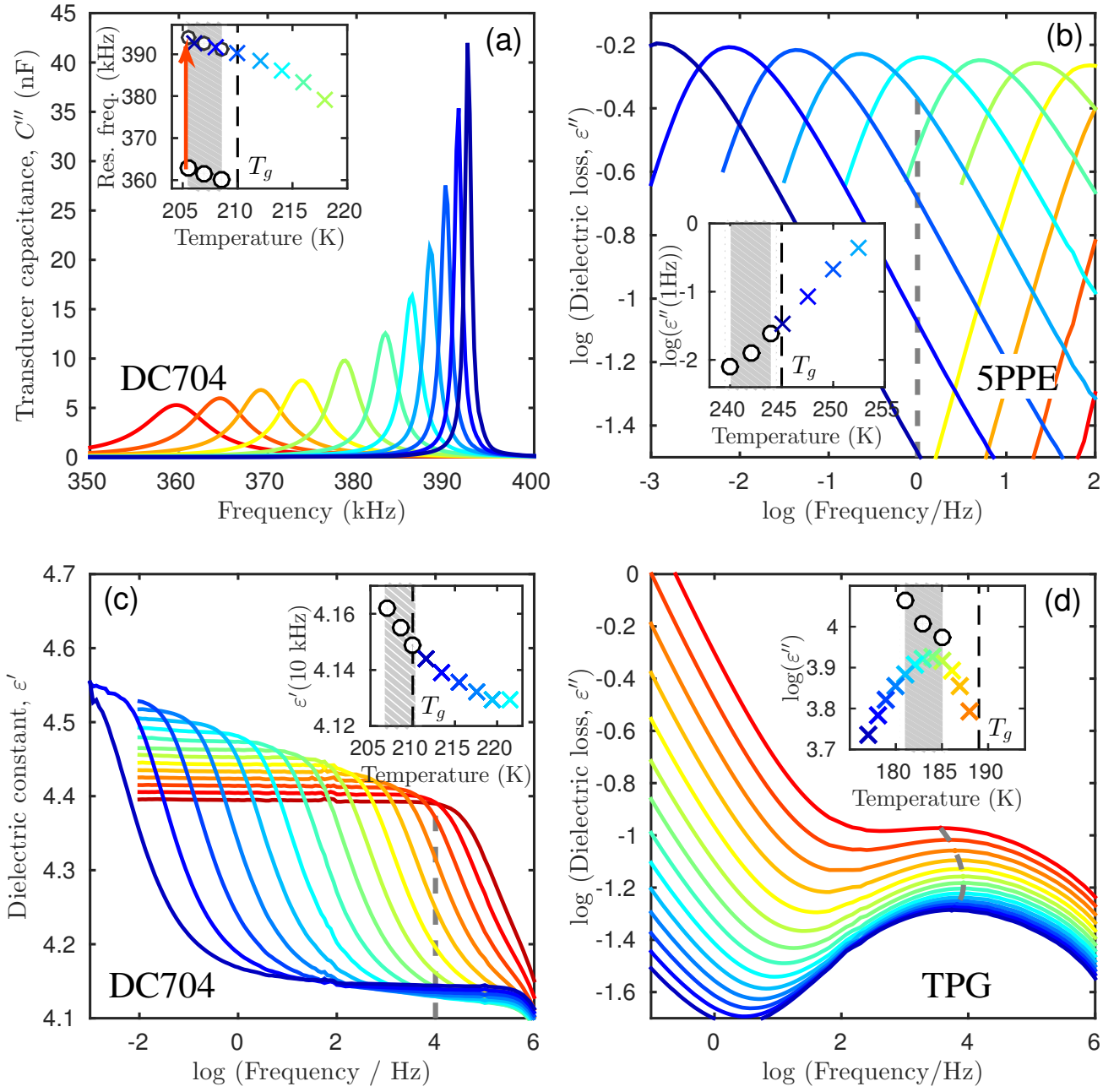

FIG. 1. Examples of the different types of data used, (a) mechanical resonance, (b) logarithm of the dielectric loss, (c) real part of the dielectric constant, and (d) logarithm of the loss-peak frequency of the (dielectric) beta relaxation. Grey dashed lines in (b,c,d) indicate the quantity being monitored during aging. In (a) it is the resonance frequency given by the peak frequency of imaginary part of the capacitance (the method used for determining this frequency is described in the text). The insets show this quantity as a function of temperature, in which the grey area indicates the range of temperatures involved in the aging measurements. The black circles show the equilibrium values of the measured quantity after annealing. For the two dielectric quantities (b and c), the aging points continue the equilibrium values measured above T_g. For the mechanical resonance (a), the aging points are shifted towards lower frequencies because the equilibrium scans are from a different set of measurements, and the resonance frequency varies with the degree of filling and the specific piezo-electric disc used. When these aging data points are shifted (arrow in the inset of (a)), they too continue on the line from the equilibrium measurements.

Liquid	T_g (K)	T_0 (K)	ΔT (K)	Probe	X_0	$\Delta X_{up}/\Delta X_{down}$	$\lvert a\rvert$*	Ref.
DC704	210	207	1.5	f_{res}/kHz (mech.)	361.4	1.292/-1.438	261	this work
TPP	203	198.3	0.6	f_{res}/kHz (mech.)	464.6	0.9755/-0.9837	130	this work
DC704	210	208.5	1.5	ϵ'(10 kHz)	4.1553	6.157/-6.457 ($\times 10^{-3}$)	875	this work
5PPE	245	242	2.0	$\log[\epsilon''(1\text{ Hz})]$	-1.89	-0.215/0.277	8.5	1
TPP	203	200	2.0	$\log[\epsilon''(1\text{ Hz})]$	-1.95	-0.373/0.453	9.5	1
DEP	185	183	1.0	$\log[\epsilon''(1\text{Hz})]$	-0.686	-0.153/0.167	4.4	1
2,3-epoxy	190	188	2.0	$\log[\epsilon''(0.37\text{Hz})]$	-1.158	-0.373/0.412	6.0	1
DBP	177	176	1.0	$\log[\epsilon''(0.18\text{ Hz})]$	-0.749	-0.212/0.206	3.8	1
TPG	189	183	2.0	$\log\left[f_{\beta,max}/\text{Hz}\right]$ (diel.)	4.009	3.4/-5.3 ($\times 10^{-2}$)	47	2

*) determined from Eq. (9)

TABLE I. Overview of all liquids studied.

where ω is the angular frequency. This may be rewritten as

$$J = \frac{C}{1 + i\frac{\omega}{\omega_0}\frac{1}{Q} - \left(\frac{\omega}{\omega_0}\right)^2} \tag{3}$$

where $\omega_0 = \frac{1}{\sqrt{LC}}$ is the angular resonance frequency, and $Q = \frac{1}{R}\sqrt{\frac{L}{C}}$ is the standard resonance quality factor. If there is a sharp resonance ($Q \gg 1$), J is approximately given by

$$J \approx \frac{C}{1 - \left(\frac{\omega}{\omega_0}\right)^2} \tag{4}$$

which gives the purely imaginary impedance

$$Z = \frac{1}{i\omega J} \approx \frac{1}{i\omega C}\left(1 - \left(\frac{\omega}{\omega_0}\right)^2\right). \tag{5}$$

This expression implies that the impedance is zero at the resonance frequency, $Z(\omega = \omega_0) = 0$.

Measuring at two frequencies close to the resonance, (ω_1, J_1) and (ω, J_2), we can determine the resonance frequency ω_0 precisely by the following relation based on Eq. (5)

$$\omega_0 = \sqrt{\frac{\omega_2^2 - A\omega_1^2}{1 - A}}, \quad A = \frac{Z_2''\omega_2}{Z_1''\omega_1} \tag{6}$$

from which the resonance frequency is given as $f_{res} = \omega_0/2\pi$.

In Fig. 3 the principle is demonstrated in the case of DC704. The figure shows the two measured frequencies (blue and pink lines) and the inferred resonance frequency, f_{res} (black dots). The figure demonstrates the high resolution of this measurement.

B. Low-frequency dielectric loss, $\epsilon''(1\text{ Hz})$

These data were published in Ref. 1 and have been reanalyzed here. The measurements were carried out with a two-disc capacitor in contact with a Peltier element. The concept is described in detail in Ref. 3. The liquid layer is 50 μm thick and the use of a Peltier element minimizes heat diffusion lengths outside of the liquid layer. This geometry and the thin liquid layer minimize the characteristic thermal equilibration time when changing temperature to a mere two seconds. The set temperature may be kept constant over weeks within 100 μK.

Aging was studied by monitoring the dielectric loss at a fixed frequency as a function of time following a temperature jump. The monitoring frequency f is much larger than the loss-peak frequency, but f must be sufficiently below any contributions from potential beta processes. These constraints vary with the liquid and the selected temperature range, and the choice of f was optimized for each liquid [1].

C. High-frequency dielectric constant, $\epsilon'(10\text{ kHz})$

The high-frequency dielectric measurements were performed under same conditions and with the same type of cell as the low-frequency dielectric loss described above, except that the monitoring frequency in this case was 10 kHz.

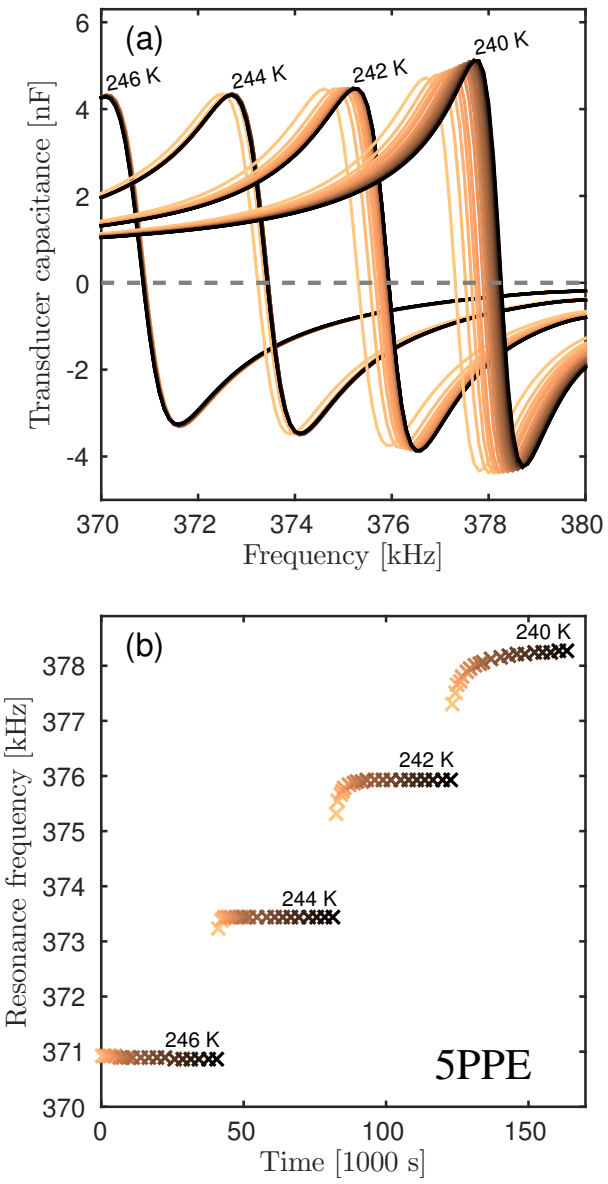

FIG. 2. (a) Series of frequency scans across the resonance for four temperatures (data for 5PPE). As the temperature is decreased, the liquid stiffens and gets harder, and the resonance moves to higher frequencies. In (b) the resonance frequency found from data in (a) is plotted as a function of time. At the highest temperature (246 K), the curve is flat, reflecting that the sample is in equilibrium almost immediately. With lower temperatures equilibration takes progressively longer time. At the lowest temperature (240 K) equilibrium is not reached in this measurement.

D. Beta loss-peak frequency aging, $f_{\beta,max}$

The beta loss-peak frequency aging data were published in Ref. [2], but not reported as functions of time because that publication focussed on the relation during aging between the beta loss-peak frequency and maximum loss. These are the only data of the paper that

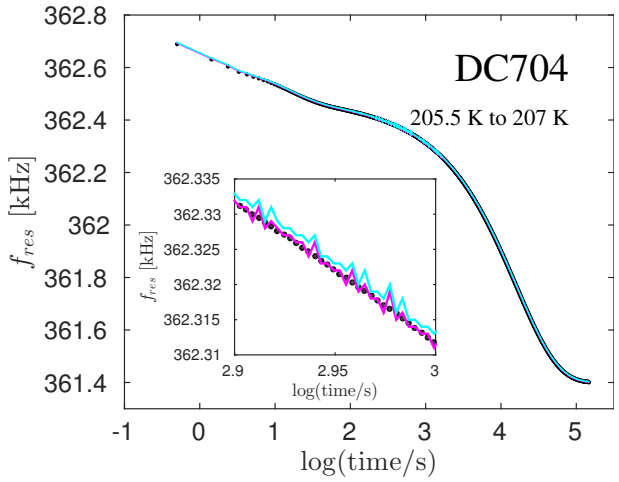

FIG. 3. Example of how the resonance frequency is determined from two measured points. The two measured frequencies are shown in pink and blue and the inferred resonance frequency (see Eq. (6)) in black circles. The inset shows a zoom of the full curve. Even if the two measured frequencies have some jitter, the calculated resonance frequency follows a smooth curve with nearly no noise.

do not utilize the fast and accurate sub-cryostat with the Peltier element. The monitored property is the peak position of the beta relaxation, so each point on the aging curve requires a full frequency scan of the beta peak region. Thus, both the scanning time and the thermal equilibration time are much longer than in the other measurements. Consequently, to make it possible to approximate a complete temperature jump, the annealing temperature for this sample is further below T_g (and the time to reach structural equilibrium longer) than for the other data sets. Thus these aging data are 6 K below the glass transition temperature, whereas the other sets are 2-3 K below.

The peak position was determined as the top point of a second order polynomium fitted to 9 data highest data points in the beta region, involving a frequency range of 0.5 decades.

The protocol for the measurement is jumping in steps of 2 K from 185 K to 181 K and back up in temperature. For the lowest temperature the sample was not fully equilibrated before the temperature was raised again. To properly estimate the equilibrium values necessary for the analysis and tests of the theory, we invoked time-aging time superposition as well as time-temperature superposition, making it possible to build the full relaxation curve from the different pieces at different temperatures. Thus the data of the paper are based on the 185 K to 183 K down jump and the 183 K to 185 K up jump.

For shifting on the time axes, we used the extrapolations of the equilibrium relaxation rate shown in Fig. 4, assuming that the structural equilibration time is proportional to the dielectric relaxation time given as the inverse alpha loss-peak frequency. Then the curve was

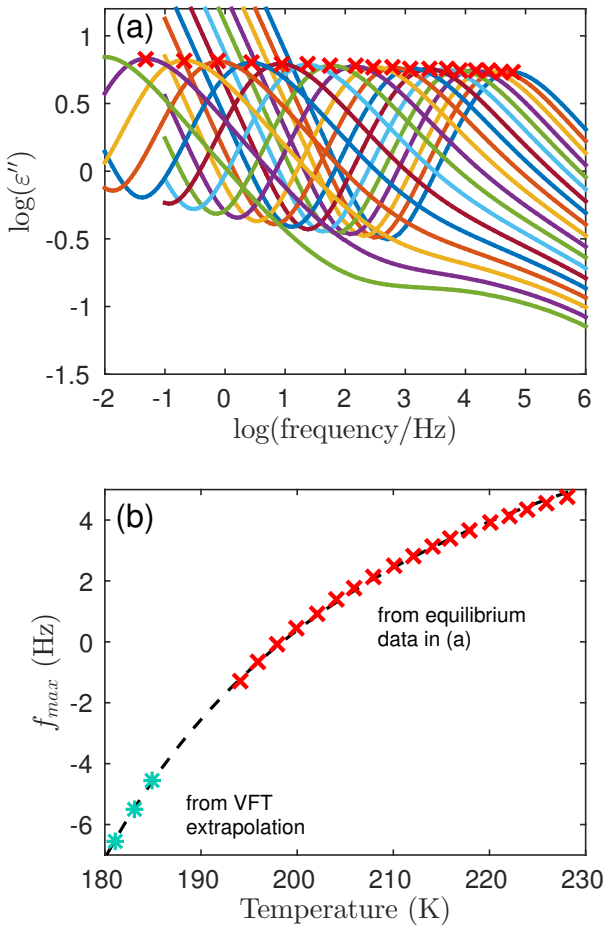

FIG. 4. (a) Dielectric relaxation spectra of TPG with the alpha peak position marked by a red cross measured at temperatures much above those where aging was studied (181-185 K). (b) Peak positions as a function of temperature. The black dashed line represents a VFT extrapolation of the peak frequency down to the annealing temperatures of the aging experiment. The annealing temperatures are marked by grey horizontal lines; the intersection of the VFT extrapolation and these lines gives the predicted/extrapolated equilibrium relaxation rates at the annealing temperatures.

shifted of the y-axes to get the best overlap with the relaxation measured at that temperature. Measured and shifted curves are shown in Fig. 5. Measured data points are plotted with asterices, while shifted curves are plotted with dots in the same color as the original data points.

III. THE a PARAMETERS

For the tests of the two predictions of the single-parameter theory given in Figs. 3 and 4 of the paper the constant a for each sample needs to be determined.

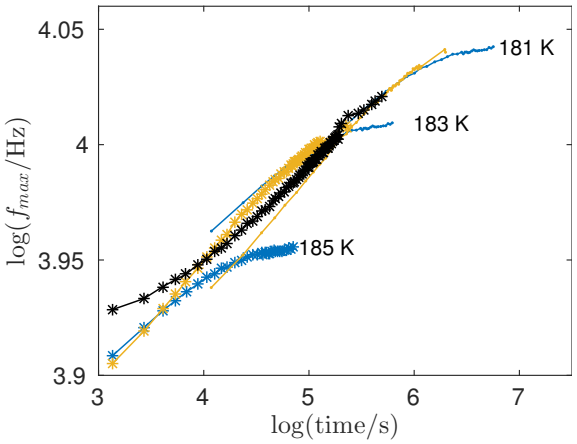

FIG. 5. Left: Logarithm of the beta loss-peak frequency of TPG as a function of time for the three temperature down jumps. The measured aging curves are plotted with asterices, shifted (see text) curves with dots in the same color as the original data points. Note that the instantaneous change in the beta loss-peak frequency is in the opposite direction compared to the subsequent aging.

Prediction 1:

$$\ln\left(-\frac{\dot{R}}{\gamma_{\rm eq}}\right) - a\frac{\Delta X(0)}{X_0}R = \ln\left(F(R)\right) \tag{7}$$

Prediction 2:

$$t_2(R) = \int_0^{t_2(R)} dt_2 = \int_0^{t_1(R)} \exp\left(\Lambda_{12}R(t_1)\right)\, dt_1 \tag{8}$$

where $\Lambda_{12} = a(\Delta X_1(0) - \Delta X_2(0))/X_{\rm eq}$.

In principle, a could be treated as a free parameter. Below we present two alternative methods for determining a from data, leaving zero parameters of the theory. The first one is described in Sec. III A and is used in the paper; the second one involves some extra assumptions, see Sec. III B below.

A. Determining a from aging data

In the paper we determine a empirically from the relation

$$\int_0^\infty \left(e^{\Lambda_{12}R_1(t_1)} - 1\right)\, dt_1 + \int_0^\infty \left(e^{-\Lambda_{12}R_2(t_2)} - 1\right)\, dt_2 = 0 \tag{9}$$

regarding this relation as one equation with one unknown, a.

In practice this implies numerical integration of the normalized aging data curves and minimizing the difference between the two integrals by tweaking a. Since data rarely extend to infinity, we use the relation with a

common cut-off in the relaxation function R

$$\int_0^{t_1(R)} \left(e^{\Lambda_{12} R_1(t_1)} - 1\right) dt_1 + \int_0^{t_2(R)} \left(e^{-\Lambda_{12} R_2(t_2)} - 1\right) dt_2 = 0\,. \tag{10}$$

We note that the above relation is not an approximation and that Eq. (9) is simply the limit of this for $R \to 0$.

For all liquids except TPG this cut-off was 1 %, i.e. $R = 0.01$. For the TPG data the cut-off was set higher, 6.67 %.

The constant a was found to vary by orders of magnitude with the measurement type (Fig. 7).

B. Estimation of $a_{\text{extrapolated}}$

In principle, a can be found by equilibrium measurements by invoking the chain rule

$$a = \frac{d \ln \gamma_{\text{eq}}}{d \ln X_{\text{eq}}} = \frac{d \ln \gamma_{\text{eq}}}{d \ln T} \Big/ \frac{d \ln X_{\text{eq}}}{d \ln T}\,. \tag{11}$$

The quantity $d \ln X_{\text{eq}} / d \ln T$ can be calculated directly from the aging measurements since $X_{\text{eq}} = \lim_{t\to\infty} X(t)$. For a set of an up jump and a down jump to the same temperature we have both X_{eq} and ΔX, which gives three equilibrium values of X at three temperatures.

The other quantity, $d \ln \gamma_{\text{eq}} / d \ln T$ (closely related to the fragility), is not readily obtainable from the aging measurements, because it requires knowledge of the equilibrium clock rate γ_{eq} at temperatures below T_g, which is not measured directly. If one assumes that the equilibrium clock rate is proportional to the equilibrium dielectric relaxation rate determined as the alpha loss-peak frequency, f_{max}, (an assumption rendered probable in Refs. 1 and 10), dielectric data can be used to determine $d \ln \gamma_{\text{eq}} / d \ln T$ above T_g and subsequencly extrapolated to lower temperatures.

This procedure is implemented in Fig. 6 where the temperature dependence of the alpha loss-peak frequency f_{max} of the dielectric loss and the calculated $d \ln f_{\text{max}} / d \ln T$ is shown for all the liquids studied. The latter increases with decreasing temperature [8] approaching $150 - 220$ around T_g. Note that here we did not use a VFT extrapolation for the relaxation rate. Instead, we extrapolated the calculated quantity $d \ln \gamma_{\text{eq}} / d \ln T$, as we believe this method is more likely to give reasonable extrapolations [8].

Figure 7 shows the obtained a-values from extrapolation as a function of the a values found from extrapolation. In general, the two methods give almost perfect correlation. The slight deviations reflect either that the dielectric relaxation time is not always identical to the material time or simply the challenge of extrapolating from higher temperatures.

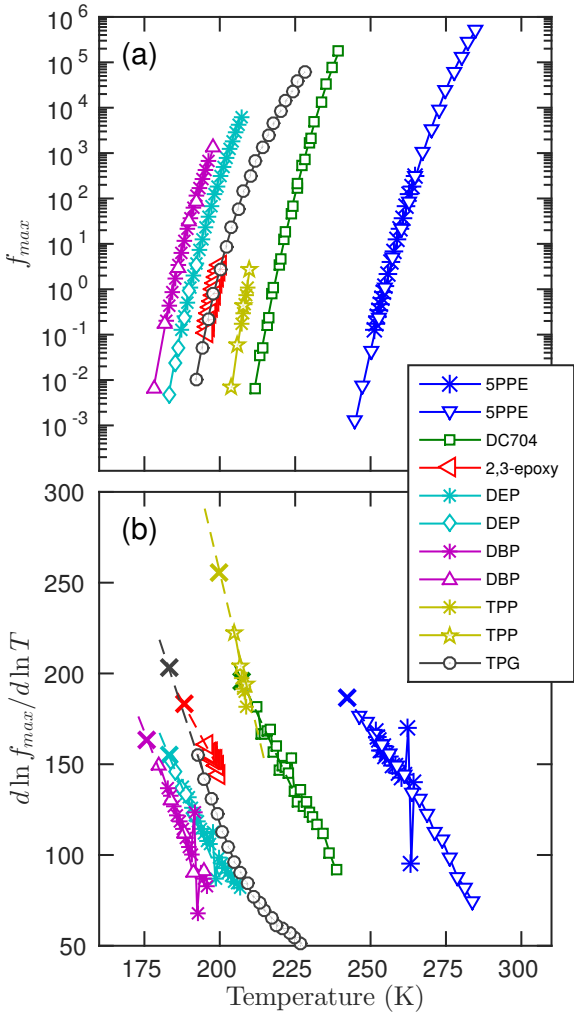

FIG. 6. (a) Relaxation map of the dielectric loss peaks (γ_{eq}) for the liquids used in this work. Data are from [1, 8–10]. (b) The logarithmic derivatives of the relaxation frequencies. The dashed lines represent the extrapolations, the crosses mark the aging temperatures.

IV. TESTING PREDICTIONS 1 AND 2 FOR OTHER DATA

Figure 8 shows the two predictions (Eq. (7) and (8)) for the data not included in the paper.

Prediction 1 works well for all liquids and measurement types. Prediction 2 predicts curves that show some deviations from the data at the short times for the dielectric loss, whereas the mechanical resonance gives a perfect overlap. This is difficult to see on the full curve because the temperature jump is small ($\Delta T = 0.6$ K), but the inset shows the overlap when zooming in on part of the curve. The deviations for the dielectric loss data is worse for those liquids that have a strong beta process. These deviations may thus be due to interference from the beta process.

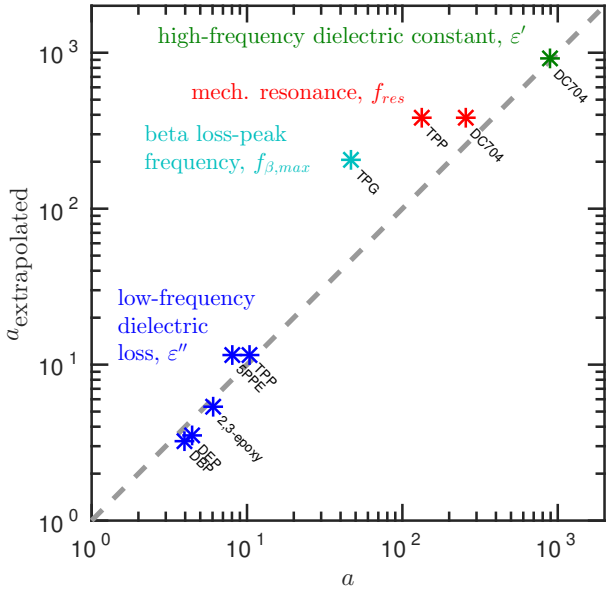

FIG. 7. Comparison of the a value determined from data via Eq. (9) and that estimated via Eq. (11) by extrapolation of the equilibrium dielectric relaxation rates. The numerical value of a varies greatly with the type of measurement: for the dielectric loss data $a \sim 10^1$, for the mechanical resonance and beta loss-peak data $a \sim 10^2$, while for the high-frequency dielectric real part data $a \sim 10^3$. All low-frequency dielectric loss data of Ref. [1] are included here, as well as an extra set of mechanical resonance data (for TPP). There is good agreement between the estimated a values from extrapolation and those determined from the aging data. Deviations either reflect that the dielectric relaxation time is not always identical to the material time or simply the challenge of extrapolating from higher temperatures.

V. COMMENTS ON EQUATION (7)

Equation (7) of the main paper is a non-linear differential equation for the normalized relaxation function R

$$\dot{R} = -\gamma_{\rm eq} F(R) \exp\left(a \frac{\Delta X(0)}{X_{\rm eq}} R\right) . \qquad (12)$$

We note the following:

1. In the limit $\Delta T \to 0$ Eq. (12) becomes $\dot{R} = -\gamma_{\rm eq} F(R)$. This describes a small temperature jump for which aging is a linear-response phenomenon and the material time reduces to ordinary time. This differential equation determines the convolution kernel $M(\xi)$ of the general aging equation (Eq. (2) of the main paper). Thus, linear aging determines the general, nonlinear aging [11, 12].

2. In the long-time limit $R(t) \to 0$, $\dot{R}(t) \to 0$, and $\gamma(t) \to \gamma_{\rm eq}$. Equation (12) here also reduces to the linear-limit aging equation, $\dot{R} = -\gamma_{\rm eq} F(R)$. Clearly, $F(R) \to 0$ for $R \to 0$. The generic analytic case is $F(R) = CR$ for $R \to 0$. This leads to a simple exponential relaxation in the long-time limit, a property for which there is some experimental evidence [1]. The stretched-exponential relaxation function $R(\xi) = \exp(-\xi^\beta)$, on the other hand, which is often used to fit aging data, corresponds to the non-analytic function $F(R) \propto R(-\ln(R))^{(\beta-1)/\beta}$.

3. If $F(R) = CR$ for all R, Eq. (12) may be rewritten to become a differential equation for $\Delta X(t)$. This is a special case of the above-mentioned Tool-type aging equations [13].

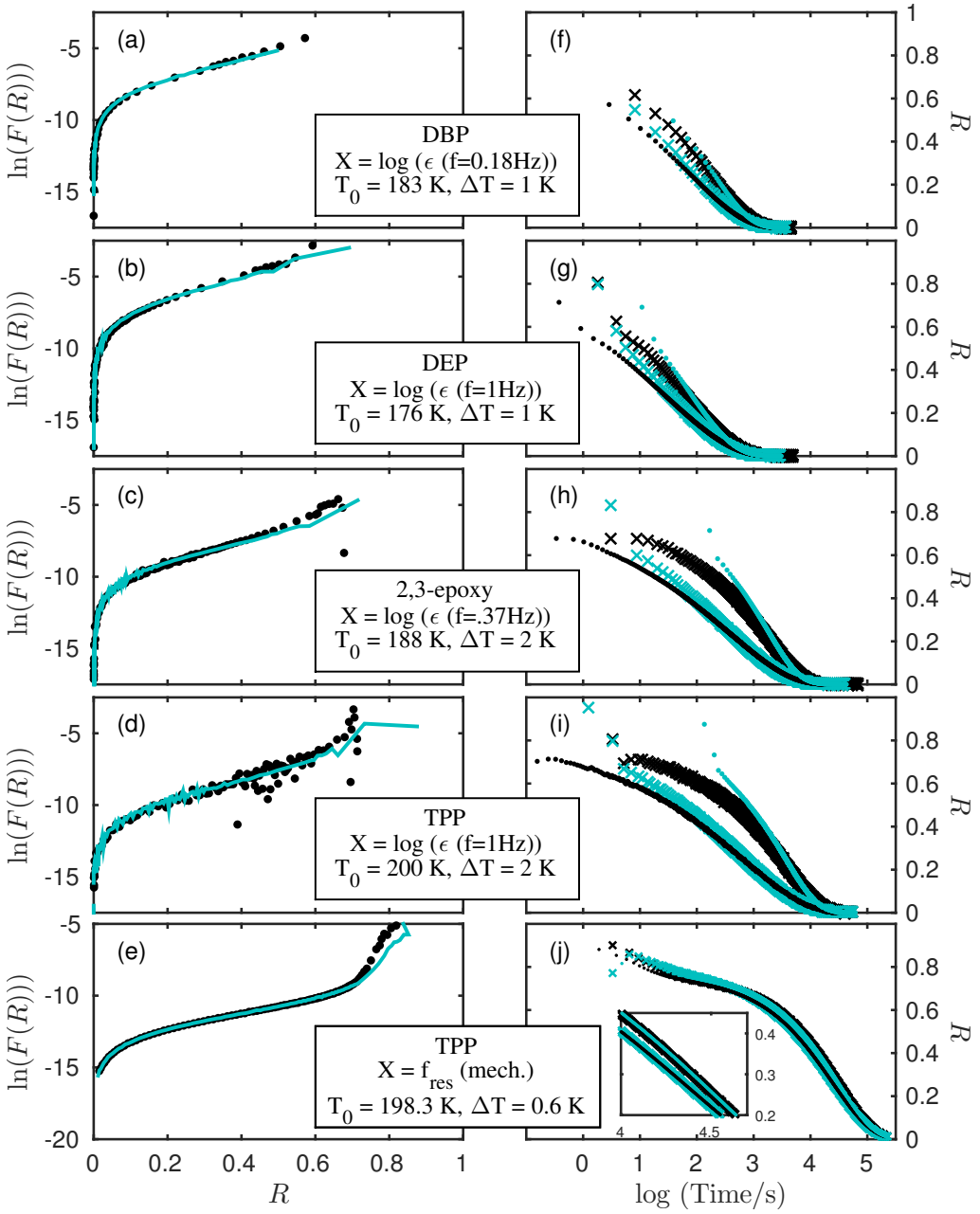

FIG. 8. Predictions from the theory for all data included in Fig. 5 of the paper not otherwise shown. (a-e) Prediction 1 for DBP (dielectric loss), DEP (dielectric loss), 2,3-epoxy (dielectric loss), TPP (dielectric loss), TPP (mechanical resonance), (f-j) Prediction 2 for the same liquids and measurement types.

[1] T. Hecksher, N. B. Olsen, K. Niss, and J. C. Dyre, J. Chem. Phys. **133**, 174514 (2010).

[2] J. C. Dyre and N. B. Olsen, Phys. Rev. Lett. **91**, 155703 (2003).

[3] B. Igarashi, T. Christensen, E. H. Larsen, N. B. Olsen, I. H. Pedersen, T. Rasmussen, and J. C. Dyre, Rev. Sci. Instrum. **79**, 045105 (2008).

[4] B. Igarashi, T. Christensen, E. H. Larsen, N. B. Olsen, I. H. Pedersen, T. Rasmussen, and J. C. Dyre, Rev. Sci. Instrum. **79**, 045106 (2008).

[5] T. Christensen and N. B. Olsen, Phys. Rev. B **49**, 15396 (1994).

[6] N. B. Olsen, J. C. Dyre, and T. E. Christensen, Phys. Rev. Lett. **81**, 1031 (1998).

[7] T. Christensen and N. B. Olsen, Rev. Sci. Instrum. **66**, 5019 (1995).

[8] T. Hecksher, A. I. Nielsen, N. B. Olsen, and J. C. Dyre, Nat. Phys. **4**, 737 (2008).

[9] A. I. Nielsen, B. Jakobsen, K. Niss, N. B. Olsen, R. Richert, and J. C. Dyre, J. Chem. Phys. **130**, 154508 (2009).

[10] B. Jakobsen, T. Hecksher, T. Christensen, N. B. Olsen, J. C. Dyre, and K. Niss, J. Chem. Phys. **136**, 081102 (2012).

[11] O. S. Narayanaswamy, J. Am. Ceram. Soc. **54**, 491 (1971).

[12] P. Lunkenheimer, R. Wehn, and A. Loidl, Phys. Rev. Lett. **95**, 055702 (2005).

[13] G. W. Scherer, *Relaxation in Glass and Composites* (Wiley, New York, 1986).